



## Monitoring of ozone production and depletion rates in a tritium-compatible system

Dominic Batzler<sup>a,\*</sup>, Max Aker<sup>a</sup>, Robin Größle<sup>a</sup>, Daniel Kurz<sup>a</sup>, Alexander Marsteller<sup>a,b</sup>, Florian Priester<sup>a</sup>, Michael Sturm<sup>a</sup>, Peter Winney<sup>a</sup>

<sup>a</sup> Tritium Laboratory Karlsruhe, Institute for Astroparticle Physics, Karlsruhe Institute of Technology, Hermann-von-Helmholtz-Platz 1, 76344 Eggenstein-Leopoldshafen, Germany

<sup>b</sup> Center for Experimental Nuclear Physics and Astrophysics, University of Washington, Seattle, WA 98195, USA

### ARTICLE INFO

#### Keywords:

Tritium decontamination  
UV  
Ozone  
Monitoring

### ABSTRACT

As surfaces are exposed to tritium, they will inevitably accumulate it, leading to the tritium memory effect. In order to reduce this effect, e.g. in analytic systems, decontamination methods are required. UV/ozone decontamination is known to be an efficient method, but its fundamental mechanism is not well known. In a dedicated UHV-compatible experiment, this method will be investigated systematically. This work focuses on the pressure dependent ozone production and depletion rates, as well as equilibrium concentration. All three properties showed a linear dependence on pressure, but showed a change in slope over time, converging to a stable level. During UV/ozone exposure, a steady increase in CO<sub>2</sub> concentration was observed in early measurements. Both effects indicate a cleaning effect of the setup's inner surfaces.

## 1. Introduction

Operating facilities with tritium creates the need for suitable decontamination strategies. This includes the reduction of tritium memory effects in analytic systems [1], tritium accounting [2], or decommissioning. The UV/ozone decontamination method is a known technique to remove a variety of contaminants from surfaces [3], that is also applicable to tritiated surfaces [4]. Aker et al. [5] tested multiple in-situ decontamination methods, e.g. baking out and evacuating, of the rear wall, a surface inside the KATRIN experiment's tritium source prone to tritium accumulation [6]. Its surface activity was continuously monitored via beta-induced X-ray spectrometry [7]. The decontamination with UV/ozone proved to be the most efficient method [5], however, the fundamental processes leading to its decontamination effect are not sufficiently understood.

To gain a better understanding of the UV/ozone decontamination and to optimize its application to tritium containing systems, the technique will be investigated systematically in a dedicated experiment. Within this work, the pressure dependent ozone production and depletion rates, as well as its equilibrium concentration will be investigated using spectroscopic methods.

## 2. The UV/Ozone (UVO) experiment

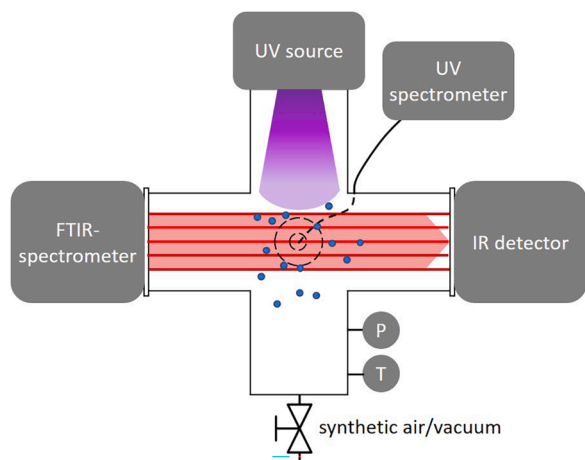
The UVO experiment was set up to investigate the underlying mechanism leading to the decontamination efficiency of the UV/ozone cleaning method. Emphasis is placed on the identification of substances in the gas phase originating from surface-bound species.

Fig. 1 shows a schematic of the experiment. The vacuum system consists of a DN 40 CF double cross-piece that serves as the sample cell, a secondary vessel for introducing substances, e.g. for calibration purposes, a gas inlet and a pump port. For ozone production, a miniZ Hg-UV lamp by RBD Instruments, with distinct emission lines at e.g. 185 and 253 nm, is used. Due to its large spectral range and the ability to detect and quantify many gaseous substances via absorption spectroscopy, a Bruker Tensor 27 FTIR-spectrometer serves the purpose to analyse the gas composition within the cell, using a rolling circle filter baseline correction as described in [8–10]. The gas species are quantified by including absorption cross sections taken from the HITRAN database [11].

Additionally, a Broadcom Qwave UV grating spectrometer connected through an optical fiber monitors the UV source. Along the sample cell, with increasing distance from the UV source, three type K thermocouples are installed on the outside surface to measure the temperature

\* Corresponding author.

E-mail address: [dominic.batzler@kit.edu](mailto:dominic.batzler@kit.edu) (D. Batzler).



**Fig. 1.** The UVO experiment, showing the central process chamber and how it is connected to the analytic systems (UV source and spectrometer, IR spectrometer) and the process gas system (pumping, gas supply, pressure sensors). Not shown in the picture are additional temperature sensors to monitor the temperature at several positions of the system and the laboratory environment.

gradient produced by the source. A 1000 Torr full scale capacitance diaphragm pressure gauge measures the pressure inside the sample cell.

### 3. Pressure dependence of ozone production and destruction timescale, and equilibrium concentration

The experimental setup was put into service by investigating ozone itself, as it appears to be a fundamental component for decontamination. To produce ozone, the previously evacuated sample cell is filled with synthetic air, in this case, a mixture of 20.5 % O<sub>2</sub> in N<sub>2</sub> to have a reproducible starting point. As an example, Fig. 2. shows a typical measurement cycle. The ozone concentration, as measured via its absorption band centered around 1043 cm<sup>-1</sup>, is shown in blue, while the intensity of the 253 nm UV radiation from the source is shown in orange. As soon as the UV source is switched on, ozone is generated due to photodissociation of molecular oxygen caused by the 185 nm emission line, with subsequent recombination. Its production can best be described by a sum of two exponential functions, of which one accounts for the increase in source intensity during warm-up. The warm-up behaviour of the UV source is revealed by the green curve in Fig. 2., displaying the intensity of a faint emission line at 365 nm, which is not absorbed by molecular oxygen, nor ozone. At some point, the ozone concentration shows a stable equilibrium level. When the UV source is switched off, the ozone decays in a simple exponential manner. From

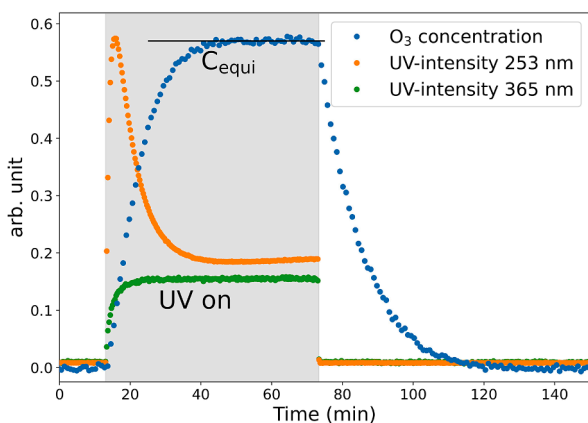


**Fig. 2.** Fundamental behaviour and interplay of ozone (blue), and the intensity of the 253 nm (orange) and 365 nm (green) UV radiation.

such a measurement, one can extract the production and decay times, defined in this work as the time after which the ozone concentration reaches  $1 - 1/e$ , or  $1/e$  of the equilibrium, respectively. During operation, the measured intensity of the 253 nm source emission line decreases significantly after its warm-up, until it stabilises. This feature can be observed due to the fact that ozone absorbs UV wavelengths around 253 nm via photodissociation. At a pressure of 1 bar, transmissions lower than 6 % with an absorption path length of around 13 cm can be measured. However, this can be exploited to have an additional, independent measurement technique to monitor ozone production and equilibrium levels.

Ozone production and depletion, as shown in Fig. 2. were measured multiple times without exchanging the gas. Similar measurements were performed at pressures ranging from 100 to 1000 mbar in 100 mbar steps and the respective production and depletion times of ozone were extracted by fitting. The result is shown in Fig. 3., which at pressures above 200 mbar shows linear behaviour both in ozone production (orange) and decay (blue) times. The production time increases from about 3.5 minutes at the lowest pressure of 100 mbar to roughly 9.5 minutes at the highest pressure of 1000 mbar, while the depletion time increases from about 2.5 minutes to about 17 minutes.

The amount of ozone in equilibrium, as shown in Fig. 4., also depends linearly on pressure, with the highest level of around 0.43 mbar partial pressure at about 1000 mbar (approx. 425 ppm) and 0.02 mbar at about 100 mbar (approx. 175 ppm). It has to be emphasised, that the data shown in Figs. 3 and 4. were taken after 9 months of ozone measurements and without contact between inner surfaces and ambient air. The very first measurements showed a significantly different slope compared to the final data, e.g. decay times of around 27 minutes at a pressure of 1000 mbar were obtained. With each subsequent ozone measurement, the pressure dependent slopes of production and depletion rates of ozone converged gradually to a reproducible value.

Similarly, while performing the measurements as shown in Fig. 3, a steady increase in CO<sub>2</sub> concentration while the UV source was switched on and ozone was produced could be observed in early data sets. To investigate this, a dedicated measurement with continuous UV illumination was taken. The result is shown in Fig. 5 and confirms the initial observation. In the course of 20 hours, over 200 ppm of CO<sub>2</sub> were produced.

The production rate gradually decreased over time after each successive UV/ozone measurement. Interestingly, no CO could be observed.

### 4. Discussion

The measured ozone lifetime of 17 min at pressures of 1 bar differs significantly from the lifetimes obtained from experiments, in which ozone-ozone interactions are investigated. In a 40 L plexiglass cylinder,

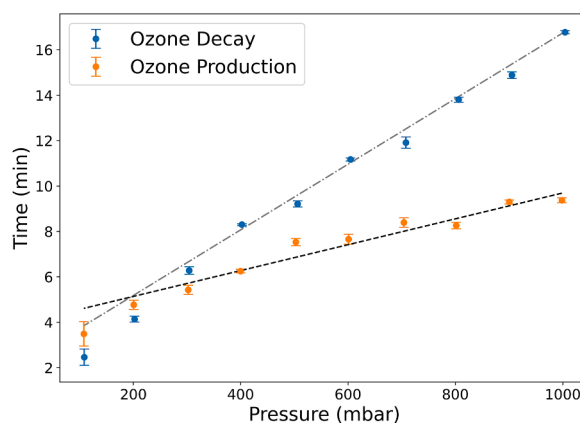


**Fig. 3.** Pressure dependence of ozone production (orange) and decay (blue) times.

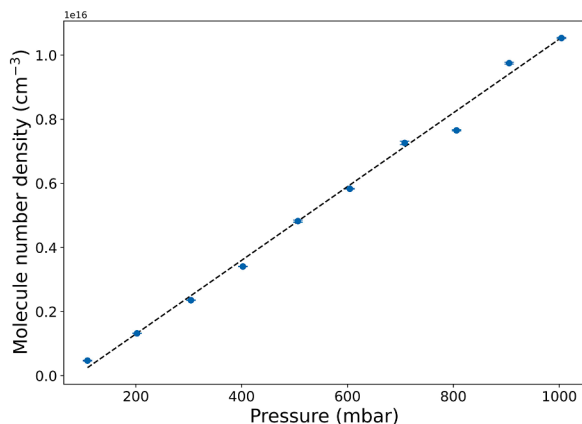


Fig. 4. Ozone molecule number density in equilibrium.

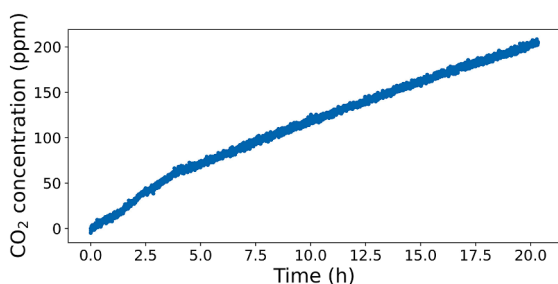


Fig. 5. Increase in CO<sub>2</sub> concentration during long-term UV source operation in early measurements.

ozone half-life times of 1524 minutes at comparable conditions were reported [12]. This indicates that primarily ozone-surface interactions are responsible for its depletion, hence, ozone lifetimes are strongly dependent on the geometry, especially the surface-to-volume ratio, of the vessel containing the ozone. Due to the large absorption of UV radiation by dioxygen and ozone, the location of the UV source might also have an effect on the decontamination efficiency. Both the gradual change in pressure dependence of the ozone properties, as well as the production of CO<sub>2</sub> during simultaneous UV illumination and ozone exposure indicates a change, or rather cleaning effect of the experiment's inner surfaces, since the amount of carbon in the gas phase at the start of each individual measurement is negligible. It has to be pointed out, that the vacuum components of the setup were not baked out and were exposed to ambient laboratory air for some months prior to usage. Hence, potential surface bound hydrocarbons, as well as the stainless steel itself, could act as a carbon source for the formation of CO<sub>2</sub>.

It would be worthwhile to test whether a UV/ozone treatment prior to commissioning is a viable in-situ conditioning method for tritium containing systems. If the carbon can be removed efficiently, the initial formation of larger amounts of tritiated hydrocarbons, e.g. tritiated methane, could be prevented.

## 5. Conclusion and outlook

The UVO experiment was planned and set up to research the fundamental mechanisms behind the UV/ozone decontamination method in order to optimise its application to tritium containing facilities, e.g. to reduce memory effects. As the first objective, in-situ ozone production and depletion rates, as well as the equilibrium concentration were studied at different pressures. In all three properties, a linear pressure dependence was measured. Together with the observed initial formation of CO<sub>2</sub> during simultaneous UV illumination and ozone

exposure, this hints towards ozone-surface interactions being a dominant effect. Hence, a UV/ozone cleaning might potentially be applied to new tritium carrying systems to deplete their carbon reservoirs before operation.

The impact of UV/ozone exposure on deuterated surfaces will be investigated next, in order to gain knowledge about the chemical form, in which deuterium is released from the surface. Finally, the measurements will be extended to also include tritium.

## CRediT authorship contribution statement

**Dominic Batzler:** Data curation, Formal analysis, Investigation, Methodology, Project administration, Software, Validation, Visualization, Writing – original draft, Writing – review & editing, Conceptualization. **Max Aker:** Conceptualization. **Robin Größle:** Conceptualization, Methodology, Resources, Software, Supervision, Writing – review & editing. **Daniel Kurz:** Formal analysis, Investigation, Writing – review & editing. **Alexander Marsteller:** Conceptualization, Software, Writing – review & editing. **Florian Priester:** Conceptualization, Resources. **Michael Sturm:** Conceptualization, Resources. **Peter Winney:** Formal analysis, Investigation, Software, Validation, Data curation.

## Declaration of competing interest

The authors declare that they have no known competing financial interests or personal relationships that could have appeared to influence the work reported in this paper.

## Data availability

Data will be made available on request.

## Acknowledgements

The authors would like to thank the tritium processing group of the Tritium Laboratory Karlsruhe for their support regarding vacuum related hardware.

We acknowledge the support of the Helmholtz Association (HGF) and the Deutsche Forschungsgemeinschaft DFG (Graduate School 1085 – KSETA), Germany.

## References

- [1] W. Bernstein, R. Ballentine, Gas phase counting of low energy beta-emitters, *Rev. Sci. Instrum.* 21 (2) (1950) 158–162.
- [2] T. Tanabe, *Tritium: Fuel of Fusion Reactors*, Springer, Tokyo, 2017.
- [3] J.R. Vig, UV/ozone cleaning of surfaces, *J. Vac. Sci. Technol. A* 3 (3) (1985) 1027–1034.
- [4] J.P. Krasznai, R. Mowat, UV/ozone treatment to decontaminate tritium contaminated surfaces, *Fusion Technol.* 28 (3P2) (1995) 1336–1341.
- [5] M. Aker, M. Sturm, F. Priester, S. Tirolf, D. Batzler, R. Größle, A. Marsteller, M. Röllig, M. Schlösser, In situ tritium decontamination of the KATRIN rear wall using an ultraviolet/ozone treatment, *Fusion Sci. Technol.* 80 (3–4) (2023) 303–310.
- [6] Aker, "KATRIN: status and prospects for the neutrino mass and beyond, *J. Phys. G* 49 (10) (2022) 100501.
- [7] M. Röllig, F. Priester, M. Babutzka, J. Bonn, B. Bornschein, G. Drexlin, S. Ebenhöch, E.W. Otten, M. Steidl, M. Sturm, Activity monitoring of a gaseous tritium source by beta induced X-ray spectrometry, *Fusion Eng. Des.* 88 (6–8) (2013) 1263–1266.
- [8] I.K. Mikhailyuk, A.P. Razzhivin, Background subtraction in experimental data arrays illustrated by the example of Raman spectra and fluorescent gel electrophoresis patterns, *Instrum. Exp. Tech.* 46 (6) (2003) 765–769.
- [9] S. Mirz, R. Groessle, A. Kraus, Optimization and quantification of the systematic effects of a rolling circle filter for spectral pre-processing, *Analyst* (2019) 4281–4287.

- [10] R. Grössle, B. Bornschein, A. Kraus, S. Mirz, S. Wozniowski, Minimal and complete set of descriptors for IR-absorption spectra of liquid H<sub>2</sub>-D<sub>2</sub> mixtures, *AIP Adv.* 10 (5) (2020).
- [11] I. Gordon, L. Rothman, R. Hargreaves, R. Hashemi, E. Karlovets, F. Skinner, E. Conway, C. Hill, R. Kochanov, Y. Tan, P. Wcislo, A. Finenko, K. Nelson, P. Bernath, M. Birk, V. Boudon, A. Campargue, K. Chance, A. Coustenis, B. Drouin, The HITRAN2020 molecular spectroscopic database, *J. Quant. Spectrosc. Radiat. Transf.* 277 (2022) 107949.
- [12] J. McClurkin, D. Maier, Half-life time of ozone as a function of air conditions and movement, in: *Proceedings of the 10th International Working Conference on Stored Product Protection*, Estoril, Portugal, 2010.